

X-RAY EMISSION FROM CLUMP BOW SHOCKS IN MASSIVE STAR WIND FLOWS

ALEXANDER E. BURKE

Department of Physics & Astronomy, Vassar College, Poughkeepsie, NY, 12604

AND

RICHARD IGNACE

Department of Physics, Astronomy & Geology, East Tennessee State University, Johnson City, TN 37164

ABSTRACT

Recent observations have shown that the emission profiles of massive stars such as ζ Pup and ζ Ori have unusually hard x-ray emissions, and the x-ray line profiles tend to be symmetrical and only slightly blueshifted. We suggest a possible explanation for this: in the highly supersonic stellar winds that form around a massive star, locally denser regions of the wind form axially symmetric bow shock structures. We treat these denser regions as rigid spherical "clumps", and assume that they exist randomly around the star. The bow shock shape is parabolic, with temperatures along the shock in excess of 106 K, decreasing from a maximum temperature at the shock head. Taking into account stellar occultation, clump occultation, and optical depth parameters, we simulate the line profiles resulting from emission along the shock. We reasonably reproduce the main features of the observed line profiles, though some parameters, such as the speed of the clumps, remain unclear at this time.

Subject headings: stars – winds, outflows – Wolf Rayet

1. INTRODUCTION

It has been known for some time that massive stars have high mass loss rates and fast moving stellar winds. Observations of these stars, including ζ Pup and ζ Ori, by the XMM-Newton and Chandra observatories have shown line profiles with unexpectedly hard x-ray emission (Oskinova et al. 2006). Several theories regarding the production of these x-rays have arisen, and several have been ruled out. Current theories place x-ray production in the stellar winds of these stars, in contrast to the corona.

Stellar winds are the radial outflow of particles from a star. The stars we deal with emit highly supersonic winds that can reach speeds in excess of 2500 km s^{-1} .

Interaction between the luminous radiation field and the gas leads to wind driving by the absorption lines; however the driving is unstable and generates clumpy wind structuring (Lucy and White 1980). Howk et al. (2000) have suggested a mechanism to explain the peculiar star τ Sco, where clumps can form close to the star due to these instabilities in the wind. After forming, they are pushed away by the radiation of the wind until they reach a peak where the force of gravity overpowers the radiation, pulling the clump back to the star. In the model, strong shocks and x-ray emitting plasma form as the ambient wind impacts the infalling clumps.

Hydrodynamic models of the shocks show that they are approximately axially symmetric paraboloids, with temperatures decreasing from the maximum at the shock head. These temperatures are hot enough to give off the type of hard x-rays that are observed. What is peculiar about the observed profiles, however, is that the x-rays tend not to be shifted and generally symmetric.

In the following, we first describe our assumptions about the star and how emission will be calculated. Next, we show how the shock shapes and emission along the shock is calculated. Then we compute line profiles for an ensemble of shocks around the star, and consider how occultation and opti-

cal depth affect the profiles. Finally, we describe the accuracy of our model, and, in the final remarks, discuss improvements that can be made.

2. ASSUMPTIONS, FORMULAE, AND PROCEDURE

The focus of our models has been to reproduce observed emission line shapes. The fundamental assumptions about the star have to do with the equations for velocity of the wind and the equations for optical depth.

We based the wind velocity on a standard velocity law commonly used in wind models:

$$v(r) = v_{\infty} (1 - b/r)^{\gamma} \quad (1)$$

where v_{∞} is the maximum velocity of the wind (we used a value of 2500 km s^{-1}), b is a constant (we used $0.98R_{*}$), and r is the spherical radius away from the star. We used a $\gamma = 1$ in our calculations of the optical depth.

The hot gas producing the x-rays is a minor component of the interior wind. The bulk of the wind can absorb x-ray photons. Thus, the photoabsorbing optical depth of the wind was calculated using the following integral:

$$\tau = \tau_0 \int_z^{\infty} \frac{dz}{r^2 w} \quad (2)$$

where τ is the optical depth, τ_0 is a scaling parameter, z is the coordinate extending from the star to the observer where zero is at the center of the star, and $w = v(r)/v_{\infty}$ is the normalized wind velocity.

Assumptions about the shocks and clumps were based on hydrodynamic simulations. The clumps are treated as rigid spheres, with near paraboloid shocks forming in front of them (Moeckel et al. 2002). The equation for the shape of the shock in 2D is

$$G = \left(\frac{\varpi}{\varpi_0} \right)^{\beta} - z_0 \quad (3)$$

where ϖ is a cylindrical radius from the z -axis, β is simply a power (we use 2 in our simulation), z_0 is the distance from the center of the clump to the shock head, and ϖ_0 is the cylindrical radius of the shock (in the direction) from the center of the clump. The full 2D shock surface derives from rotating this parabola about the z axis. We assume that X-ray emitting plasma is blown tangent to the shock by the wind, so the velocity vector for the hot gas is set by the shock jump conditions at the shock.

Line profiles were generated by determining the emission and velocity as a function of position on the shock surface, computing and binning the line flux. The total emission for an optically thin emitting gas is related to the emission measure:

$$EM = \int n^2 dV \quad (4)$$

where n is the number density of the wind, and the integral is taken over the hot gas volume.

Equally important is the differential emission measure with respect to temperature. The hydro simulations reveal this distribution to be

$$\frac{dEM}{dT} = EM_0 \left(\frac{T}{T_0} \right)^{-7/3} \quad (5)$$

where EM_0 sets the total emission measure from the entire shock, T is the temperature at some point on the shock, and T_0 is the maximum temperature at the shock head. The temperature along the shock is calculated as follows:

$$T = T_0 \left[1 + \left(\frac{dG}{d\varpi} \right)^2 \right] \quad (6)$$

Thus the total flux for each observed velocity bin in the line profile is the weighted sum of the emission for each volume bin:

$$F_{\text{bin}} = \frac{1}{D^2} \sum_T \sum_{\phi} W_{\nu} \Lambda(T) \frac{dEM}{dT} \Delta T \Delta \phi \quad (7)$$

where $\Lambda(T)$ is the cooling function, W_{ν} is a weighting function, and $\Delta \phi$ is the step size in azimuth around the shock.

Clump placement was random, and control parameters for the model include T_0 , τ_0 , EM_0 , the viewing inclination, number of clumps, and v_{∞} . Raw data was processed using convolution to simulate the resolution limitations of current detectors, simulating an observed profile.

3. RESULTS

We are trying to show that our model line profile for clump bow shocks is close in shape to the observed profiles that are symmetric, yet very slightly blueshifted from line center. In order to do this, we first considered the profile of a non-occulted, optically thin wind, with a homogeneous spread of bow shocks at a fixed radius of $2R_*$. This produces a flat top profile, as seen in the top graph of Figure 1.

The middle and bottom graphs, respectively illustrate the effects of stellar occultation and optical depth. As you can see, stellar occultation is a relatively minor effect, cutting off mainly the most redshifted emission from the profile. The bulk of emission can be blocked by the photoabsorption of the wind. As in Figure 2 photoabsorption absorbs more redshifted emission than blueshifted, creating the peak-like structure:

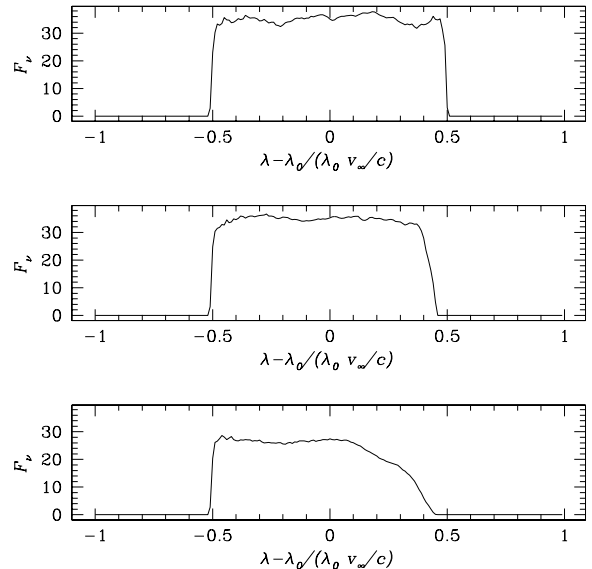


FIG. 1.— Succession of profiles illustrating the effects of stellar occultation (middle) and optical depth (bottom) on a flat-top profile (top).

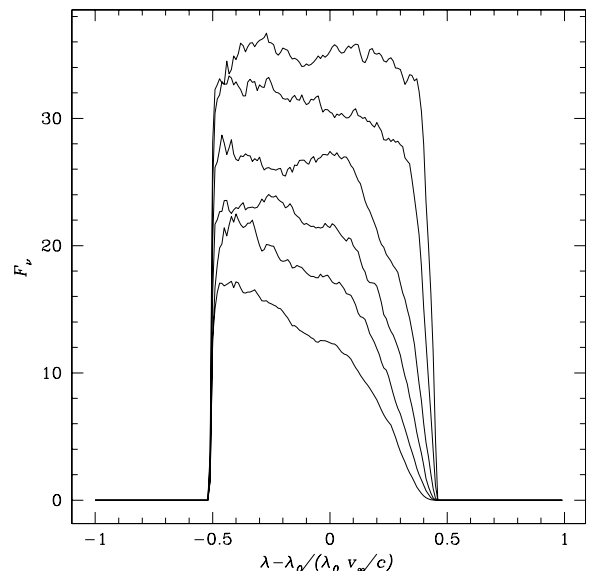


FIG. 2.— This illustrates the effects of different τ_0 values on the flat top profile. The profiles represent τ_0 values of 0, 0.1, 0.3, 0.5, 0.7, and 1, from largest to smallest.

These profiles illustrate the combined effects that optical depth and stellar occultation can have on the profile when the radius of the clumps is fixed. The variable radius profile without these parameters would look more like a symmetric peak about line center, due to the clumps appearing at different radii, thereby sampling different wind densities. Occultation and photoabsorption shape the variable radius profile into the symmetric and blueshifted profile that has been absorbed. This only occurs, however, when clumps are homogeneously distributed. To achieve this, a large number of clumps must be used, making it an important factor in determining the profile shape.

One of the most successful aspects of our model was the effect of the number of clumps on the shape of the profile.

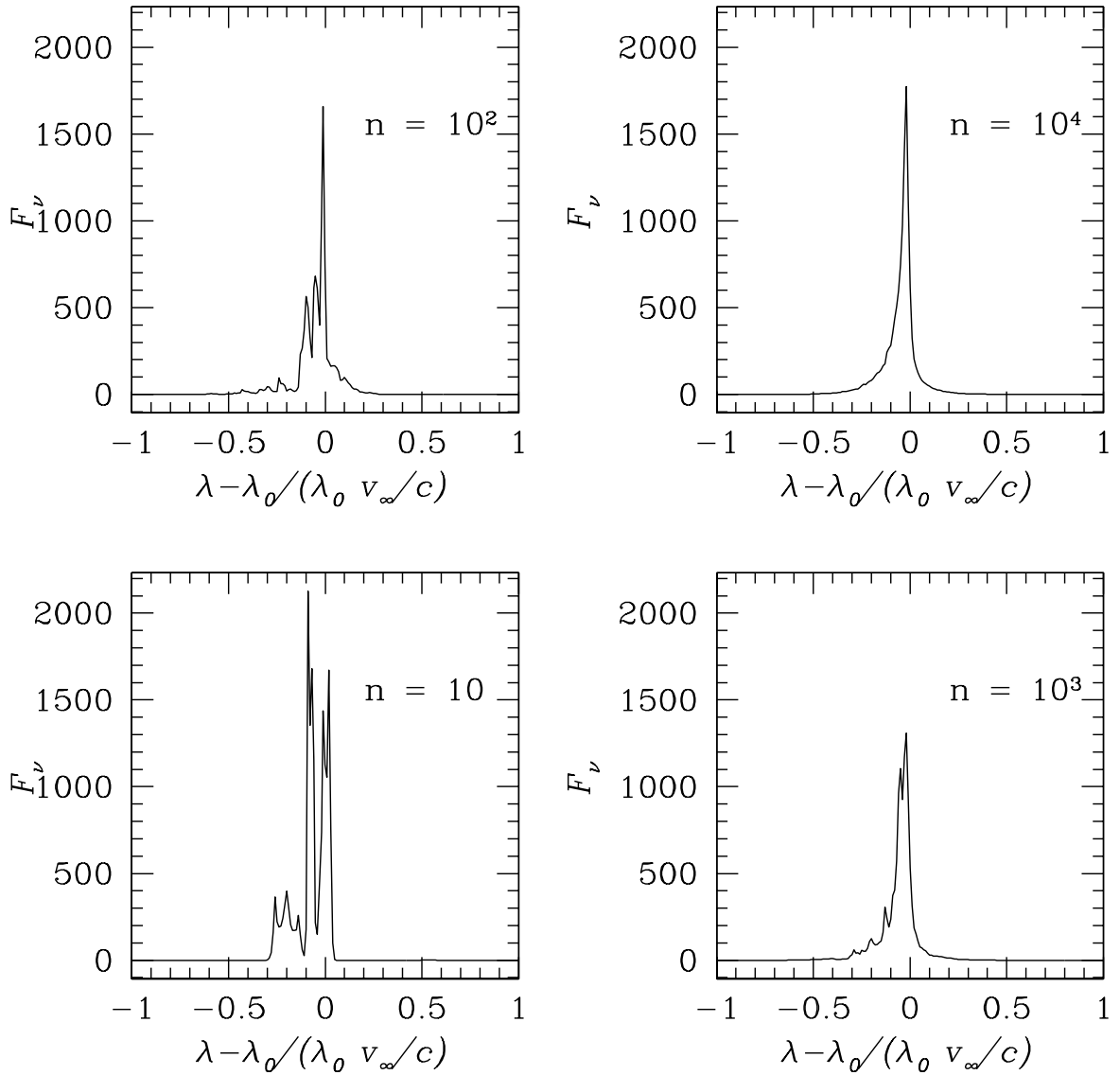


FIG. 3.— Each graph is a line profile generated using a different number of clumps as given by n .

We found that we needed to run a model with $\sim 10^4$ clumps to get a smooth profile. This suggests that clumps are not rare occurrences around these stars, and that they must form in large numbers and exist for some time in the wind. The effects of clump number are illustrated in Figure 3.

Despite the change in profile shape with different clump numbers, the profiles stay relatively consistent in both size and shape as long as a sufficient number of clumps are used. This is due to the radial distribution of clumps around the star. With a larger number of clumps there is a larger distribution of velocities for the emission from the shocks, creating a smoother profile. However, once a large number of clumps is used, the shape stays more or less the same in size and width. Figure 4 shows the thickness of the profile shapes as ten models with the same constraints are overlaid on each of the different graphs. As expected, the larger n results in less variation.

4. DISCUSSION AND FUTURE PLANS

Our model x-ray profiles have the same characteristics described by Cohen et. al. (2006): symmetric and slightly blueshifted. This suggests that the clump bow shock model of x-ray emission is promising, however there is still much work to be done. More precision work can be done on the modeling code allowing it to fit observed emission profiles accurately, rather than simply emulate the shape. Our project, however, shows promise by demonstrating the value and validity of this theory.

Funded by a partnership between the National Science Foundation (NSF AST-0552798) Research Experiences for Undergraduates (REU) and the Department of Defense (DoD) ASSURE (Awards to Stimulate and Support Undergraduate Research Experiences) programs.

REFERENCES

Carroll, B. W., & Ostlie, D. A., *An Introduction to Modern Astrophysics*, Addison-Wesley Publishing, 1996, 52, 68, 81-82

Canto, J., & Raga, A. 1998, *MNRAS*, 297, 383
Canto, J., Raga, A., & Wilkin, F.P. 1996, *ApJ*, 469, 729

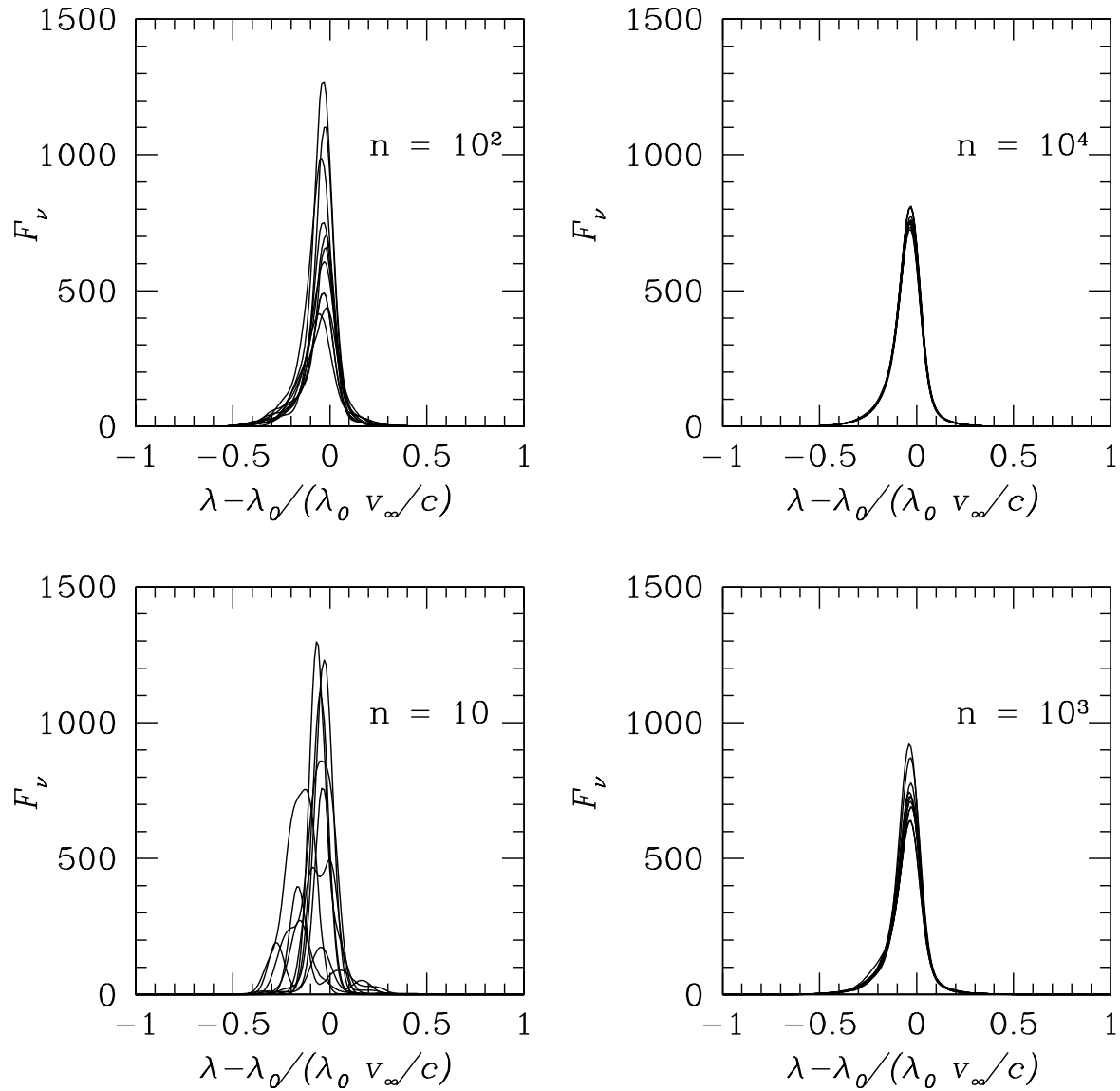


FIG. 4.— Profile shapes with Gaussian convolution to simulate detector response as achievable by the Chandra observatory instrumentation.

Cohen, David H., Leutenegger, Maurice A., Grizzard, Kevin T., Reed, Catherine L., Kramer, Roban H., & Owocki, Stanley P. 2006, MNRAS, 368, 1905
 Howk, J. Christopher, Cassinelli, Joseph P., Bjorkman, Jon E., and Lamers, & Henny J. G. L. M. 2000, ApJ, 534, 348
 Ignace, R. 2001, ApJ, 549, 119

Lucy, L. B., & White, R. L. 1980, ApJ, 241, 300
 Oskinova, L. M., Feldmeier, A., & Hamann, W.-R. 2004, A&A, 422, 675
 Oskinova, L. M., Feldmeier, A., & Hamann, W.-R. 2006, MNRAS, 372, 313
 Owocki, Stanley P., & Cohen, David H. 2001, ApJ, 559, 1108